Technical Notes

TECHNICAL NOTES are short manuscripts describing new developments or important results of a preliminary nature. These Notes cannot exceed 6 manuscript pages and 3 figures; a page of text may be substituted for a figure and vice versa. After informal review by the editors, they may be published within a few months of the date of receipt. Style requirements are the same as for regular contributions (see inside back cover).

Force Coefficients for a NACA-0015 Airfoil Undergoing Constant Pitch Rate Motions

J. H. Strickland*
Sandia National Laboratories
Albuquerque, New Mexico
and
G. M. Graham†
Ohio University, Athens, Ohio

Introduction

UTILIZATION of enhanced lift and drag coefficients produced by unsteady aerodynamics is key to the development of "supermaneuverable" flight vehicles. The supermaneuverability concept, as discussed by Herbst,[1] demonstrates the enhanced weapons delivery capability of a supermaneuverable fighter aircraft. An important unsteady aerodynamic phenomenon associated with the concept is one of a lifting surface that generates large lift and drag coefficients by a rapid pitching motion to high angles of attack ($\alpha > 45$ deg). The present investigation provides baseline experimental data for a NACA-0015 airfoil that undergoes several different constant pitch rate motions. In the past, much of the research into unsteady airfoils has been limited to those that sinusoidally oscillate about some low mean angle of attack with low amplitude. These are typified by the studies of McCroskey and Philippe,[2] McAlister and Carr,[3] Robinson and Luttges,[4] and Martin et al.[5]

A limited amount of experimental data have been obtained for airfoils undergoing constant pitching rate motion up to moderate angles of attack of at least 30 deg. These works include the study of Harper and Flanigan,[6] who obtained force balance data on a small aircraft model pitching up to 30 deg, and the work of Ham and Young,[7] who obtained surface pressure measurements on an airfoil pitching up to 30 deg, and the work of Francis and Keesee,[8] who obtained surface pressure measurements on an airfoil pitching up to 60 deg. Deekens and Kuebler[9] obtained flow visualization data for a NACA-0015 airfoil and observed the dynamic leading-edge separation phenomenon for several low Reynolds numbers ($R < 3 \times 10^4$) and nondimensional pitching rates ($K = \dot{\alpha}c \div 2U_\infty$) up to 0.26. Daley[10] obtained leading-edge dynamic stall data for Reynolds numbers up to 3×10^5 and nondimensional pitching rates up to 0.06. Walker et al.[11] obtained flow visualization data along with some hot-wire data for a NACA-0015 undergoing constant pitch rate motions. These data were obtained for Reynolds numbers on the order of 4.5×10^4 and nondimensional pitch rates up to 0.30. The further work of Walker et al.[12] produced surface pressure distributions on a NACA-0015 experiencing constant pitch rates up to $K = 0.3$ over a range of Reynolds numbers ($47{,}500 < R < 190{,}000$) up to a 60 deg angle of attack. Strickland and Graham[13] used flow visualization data to obtain a dynamic stall inception correlation at high pitch rates that also agrees with data obtained by other investigators at lower pitch rates.

Experimental Investigation

Experimental Methods

The experimental study discussed herein was conducted on a NACA-0015 airfoil operating in a tow-tank facility at a Reynolds number of 1×10^5. The results include flow visualization data, aerodynamic force data, and surface pressure distributions for six nondimensional pitching rates of $K = 0.088$, 0.19, 0.29, 0.51, 0.71, and 0.99 ($K = \dot{\alpha}c/2u_\infty$). In each case, the motion began at zero angle of attack and terminated at 90 deg angle of attack.

Flow visualization data were obtained using a hydrogen "ladder" type of bubble wire of the kind discussed in Ref. 14. Aerodynamic lift and drag forces were obtained using strain gaged load cells and from integrated surface pressure distributions. Additional details of the experimental setup are given in Ref. 15.

Flow Visualization

Analysis of the flow visualization data reveals much about the large-scale vortical motion of the fluid. Shown in Fig. 1 are typical visualization data for a nondimensional pitch rate of $K = 0.19$. These data are also representative of that for the cases of $K = 0.088$ and 0.29. That is, the progression of events over the interval of motion is similar in all three cases, with the exception that the onset of leading-edge separation is delayed with increasing pitch rate.[13]

The onset of dynamic stall is characterized by the formation of a separation bubble near the leading edge. For a nondimensional pitch rate of $K = 0.19$, this occurs at about 44 deg angle of attack. For $K = 0.29$, on the other hand, this separation occurs at an angle of attack of about 55 deg. This delay in the onset of dynamic stall is partially due to the fact that the effective angle of attack at the airfoil leading edge decreases with increasing pitch rate. As the angle of attack increases beyond stall inception, vorticity is continuously shed from the leading edge and accumulates into a large-scale vortical system sometimes referred to as the "dynamic stall" vortex.

Surface Pressure Distributions

Also shown in Fig. 1 are the surface pressure data for a nondimensional pitching rate of 0.19. At the angle of attack of 43.8 deg, the airfoil is just below the stall threshold and a large suction peak is exhibited near the airfoil leading edge whose magnitude is far in excess of that for the static case of substall angles of attack. It can be seen that, as the airfoil enters the dynamic stall region, there is a loss of suction near the leading edge, resulting in a flattening of the pressure distribution over the topside of the airfoil. This is a characteristic of static stall as well.

Presented in part as Paper 86-0008 at the AIAA 24th Aerospace Sciences Meeting, Reno, NV, Jan. 6-9, 1986; received April 7, 1986; revision received Aug. 25, 1986.

*Member, Technical Staff, Parachute Systems Division.
†Assistant Professor, Department of Mechanical Engineering.

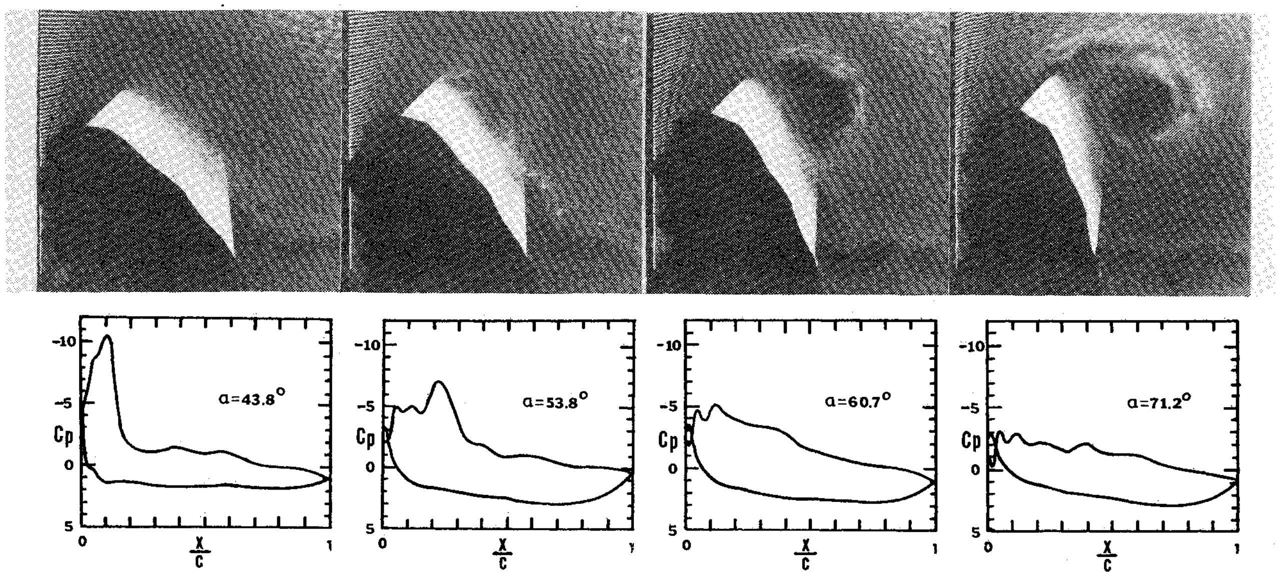

Fig. 1 Flow visualization and pressure data for $K=0.19$.

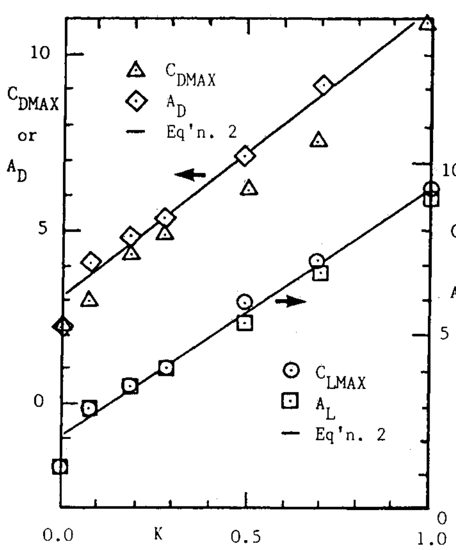

Fig. 2 Maximum lift and drag coefficients.

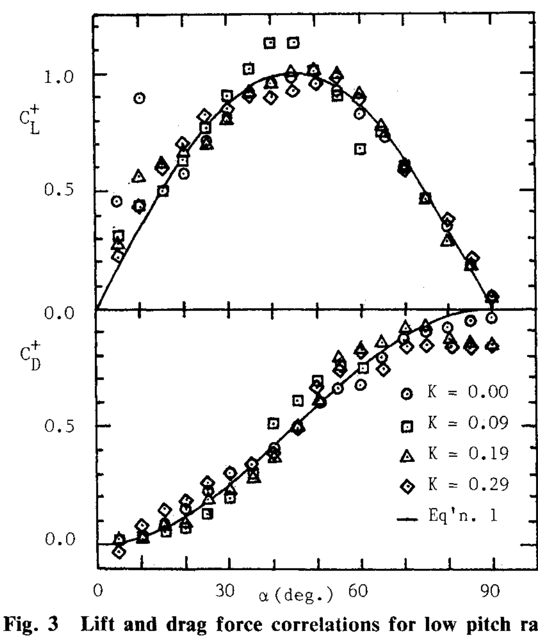

Fig. 3 Lift and drag force correlations for low pitch rates.

Lift and Drag Coefficients

Aerodynamic lift and drag forces were measured using strain gages as well as integrated surface pressure distributions. The agreement between the two measurements was, in general, within the experimental uncertainty. Only the strain gage results are presented here for the purpose of brevity.

Maximum lift and drag forces are plotted as a function of nondimensional pitching rate in Fig. 2. The data indicate an approximately linear relationship over a wide range of pitching rates.

Empirical correlations that relate the aerodynamic lift and drag forces to the pitching rate and instantaneous angle of attack may be expressed as

$$C_L(\alpha) = 2A_L \sin\alpha \cos\alpha$$

$$C_D(\alpha) = A_D \sin^2\alpha \tag{1}$$

The empirical constants A_L and A_D were determined using a least squares curve fit method to data taken at each pitching rate and are plotted in Fig. 2. Examination of Eq. (1) reveals that A_L and A_D should ideally be equal to $C_{L\max}$ and $C_{D\max}$, respectively. Equations for the solid lines are given by

$$A_L = 7.1K + 2.25 \quad (0.1 < K < 1.0)$$

$$A_D = 8.05K + 3.25 \quad (0.1 < K < 0.7) \tag{2}$$

An indication of the applicability of Eq. (1) to the test data is shown in Figs. 3 and 4. These data have been normalized as follows:

$$C_L^+(\alpha) = C_L(\alpha)/A_L$$

$$C_D^+(\alpha) = C_D(\alpha)/A_D \tag{3}$$

As may be seen in Fig. 3, the agreement between the low-to-moderate pitch rates (as well as the static case) and the simple trigonometric correlations is reasonably good over a wide range of angles of attack. The correlations begin to break down, particularly for the lift force, at the higher pitch rates, as may be seen in Fig. 4. There are undoubtedly other types of correlating functions, which might be applied over subintervals of angles of attack, that would be more accurate than the simple trigonometric ones presented here.

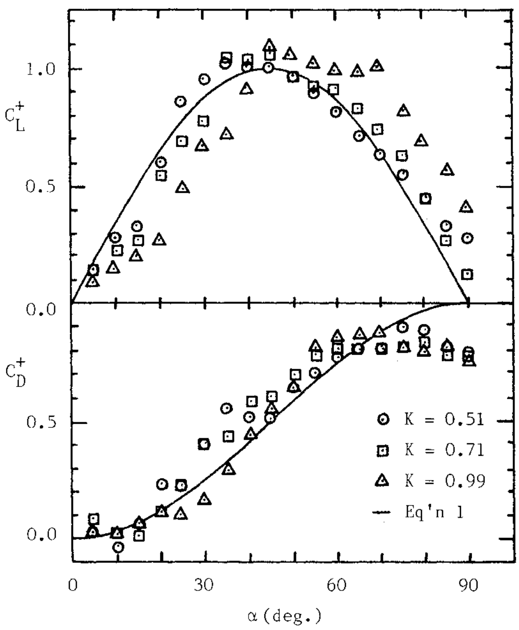

Fig. 4 Lift and drag correlations for high pitch rates.

Conclusions

Correlations for the lift and drag coefficients as a function of angle of attack and pitching rate have been obtained to a reasonable accuracy using simple trigonometric functions. Since all of the data were obtained at a single Reynolds number, using a NACA-0015 airfoil, and with an initial angle of attack equal to 0 deg, further expansion of the data base is needed.

Acknowledgment

This work was performed at the Sandia National Laboratories and was supported by the U.S. Department of Energy under Contract DE-AC04-76DP00789.

References

[1]Herbst, W., "Supermaneuverability," *Proceedings of Workshop on Unsteady Separated Flow,* U.S. Air Force Academy, Colorado Springs, CO, Aug. 1983, pp. 1–9.

[2]McCroskey, W. J. and Philippe, J. J., "Unsteady Viscous Flow on Oscillating Airfoils," *AIAA Journal,* Vol. 13, Jan. 1975, pp. 71–79.

[3]McAlister, K. W. and Carr, L. L., "Water Tunnel Visualizations of Dynamic Stall," *Journal of Fluids Engineering,* Vol. 101, Sept. 1978, pp. 376–380.

[4]Robinson, M. C. and Luttges, M. W., "Unsteady Flow Separation and Attachment Induced by Pitching Airfoils," AIAA Paper 83-0131, Jan. 1983.

[5]Martin, J. M., Empey, R. W., and McCroskey, W. J., "An Experimental Analysis of Dynamic Stall on an Oscillating Airfoil," *Journal of the American Helicopter Society,* Vol. 19, Jan. 1973, pp. 26–32.

[6]Harper, P. W. and Flanigan, R. E., "The Effect of Rate Change of Angle of Attack on the Maximum Lift of a Small Model," NACA TN2061, 1950.

[7]Ham, N. D. and Young, M. I., "Torsional Oscillations of Helicopter Blades Due to Stall," *Journal of Aircraft,* Vol. 3, May–June 1966, pp. 218–224.

[8]Francis, M. S. and Keesee, J. E., "Airfoil Dynamic Stall Performance With Large-Amplitude Motions," *AIAA Journal,* Vol. 23, Nov. 1985, pp. 1653–1659.

[9]Deekens, A. C. and Kuebler, W. R., "A Smoke Tunnel Investigation of Dynamic Separation," *Aeronautics Digest,* USAF A-TR-79-1, Feb. 1979, pp. 2–16.

[10]Daley, D. C., "The Experimental Investigation of Dynamic Stall," Thesis, Air Force Institute of Technology, Wright-Patterson AFB, Ohio, Rept. AFIT/GAE/AA/820-6, 1983.

[11]Walker, J., Helin, H., and Strickland, J., "An Experimental Investigation of an Airfoil Undergoing Large Amplitude Pitching Motions," *AIAA Journal,* Vol. 23, Aug. 1985, pp. 1141–1142.

[12]Walker, J., Helin, H., and Chou, D., "Unsteady Surface Pressure Measurements on a Pitching Airfoil," AIAA Paper 85-0532, March 1985.

[13]Strickland, J. H. and Graham, G. M., "Dynamic Stall Inception Correlation for Airfoils Undergoing Constant Pitch Rate Motions," *AIAA Journal,* Vol. 24, April 1986, pp. 678–680.

[14]Scraub, F. A., Kline, S. J., Henry, J., Runstadler, P. W., and Littell, A., "Use of Hydrogen Bubbles for Quantitative Determination of Time Dependent Velocity Fields in Low-Speed Water Flows," *Journal of Basic Engineering,* Vol. 87, June 1965, pp. 429–552.

[15]Graham, G. M., "An Experimental Investigation of an Airfoil Pitching at Moderate to High Rates to Large Angles of Attack," Ph.D. Dissertation, Texas Tech Univ., Lubbock, 1985.

Trailing-Edge Separation/Stall Alleviation

M. J. Werle,* R. W. Paterson,† and W. M. Presz Jr.‡
United Technologies Research Center
East Hartford, Connecticut

Introduction

THE overall problem addressed in this Note is that of reducing form drag due to boundary-layer separation in trailing-edge regions. As a representative application, attention is focused on airfoils at high lift conditions where, in general, loading capabilities are limited due to the occurrence of suction-surface boundary-layer separation. In such situations, the boundary layer is required to negotiate a strong adverse pressure rise as it approaches the trailing-edge region, resulting in boundary-layer separation (flow reversal). This boundary-layer separation results in a dramatic loss of lift and a drag increase as the airfoil begins to enter a stalled state.

The presence of such high lift separation/stall is difficult to predict, thus causing significant uncertainty for the design community. The consequence of overdesign is inefficient aerodynamics, whereas the cost of underdesign can be literally catastrophic. To date, nearly all mechanisms employed for overcoming these separation phenomena have been one of two types. The boundary layer has been energized either through the use of secondary air injection (slots, slats, blowing, etc.) or through the use of axial vortex generators (fins, troughs, grooves, etc.). Such devices achieve separation delay by energizing the boundary layer to overcome the adverse pressure gradients. The alternative approach described here focuses on providing a three-dimensional relief mechanism that permits the boundary layer to avoid the separation pressure rise. Presented herein is a brief description of the technical approach employed to develop this concept and initial results providing verification of the concept.

Technical Approach

The overall concept applied provides three-dimensional relief for a viscous boundary layer as it approaches a region of two-dimensional boundary-layer separation. This is accomplished by locally contouring the airfoil surface in the lateral direction, thereby establishing less unfavorable

Received Aug. 15, 1986.

*Manager of Gas Dynamics and Thermophysics. Associate Fellow AIAA.

†Manager, Experimental Gas Dynamics. Associate Fellow AIAA.

‡Consultant and Professor, Mechanical Engineering, Western New England College, Springfield, MA. Member AIAA.